

Comparison of thermal effects of stilbenoid analogs in lipid bilayers using differential scanning calorimetry and molecular dynamics: correlation of thermal effects and topographical position

With an annexed activity, Serdar Durdagi, Eleni Siapi, Carolina Villalonga-Barber, Xanthippi Alexi, Barry R. Steele, Maria Micha-Screttas, et al.

European Biophysics Journal
with Biophysics Letters

ISSN 0175-7571
Volume 40
Number 7

Eur Biophys J (2011)
40:865-875
DOI 10.1007/
s00249-011-0705-4



Your article is protected by copyright and all rights are held exclusively by European Biophysical Societies' Association. This e-offprint is for personal use only and shall not be self-archived in electronic repositories. If you wish to self-archive your work, please use the accepted author's version for posting to your own website or your institution's repository. You may further deposit the accepted author's version on a funder's repository at a funder's request, provided it is not made publicly available until 12 months after publication.

Comparison of thermal effects of stilbenoid analogs in lipid bilayers using differential scanning calorimetry and molecular dynamics: correlation of thermal effects and topographical position with antioxidant activity

Catherine Koukoulitsa · Serdar Durdagi · Eleni Siapi · Carolina Villalonga-Barber · Xanthippi Alexi · Barry R. Steele · Maria Michal-Screttas · Michael N. Alexis · Anna Tsantili-Kakoulidou · Thomas Mavromoustakos

Received: 26 December 2010 / Revised: 1 April 2011 / Accepted: 8 April 2011 / Published online: 8 May 2011
© European Biophysical Societies' Association 2011

Abstract In previous studies it was shown that cannabinoids (CBs) bearing a phenolic hydroxyl group modify the thermal properties of lipid bilayers more significantly than methylated congeners. These distinct differential properties were attributed to the fact that phenolic hydroxyl groups constitute an anchoring group in the vicinity of the head-group, while the methylated analogs are embedded deeper towards the hydrophobic region of the lipid bilayers. In this work the thermal effects of synthetic polyphenolic stilbenoid analogs and their methylated congeners have been studied using differential scanning calorimetry (DSC).

Electronic supplementary material The online version of this article (doi:10.1007/s00249-011-0705-4) contains supplementary material, which is available to authorized users.

C. Koukoulitsa · T. Mavromoustakos
Chemistry Department, University of Athens,
Zographou, 15784 Athens, Greece

S. Durdagi
Institute for Biocomplexity and Informatics,
Department of Biological Sciences, University of Calgary,
Calgary, AB, Canada

E. Siapi · C. Villalonga-Barber · B. R. Steele ·
M. Michal-Screttas · T. Mavromoustakos (✉)
Institute of Organic and Pharmaceutical Chemistry,
National Hellenic Research Foundation,
Vas. Constantinou 48, 11635 Athens, Greece
e-mail: tmavrom@chem.uoa.gr

X. Alexi · M. N. Alexis
Institute of Biological Research and Biotechnology,
National Hellenic Research Foundation,
Vas. Constantinou 48, 11635 Athens, Greece

A. Tsantili-Kakoulidou
School of Pharmacy, University of Athens,
Zographou, 15784 Athens, Greece

Molecular dynamics (MD) simulations have been performed to explain the DSC results. Thus, two of their phenolic hydroxyl groups orient in the lipid bilayers in such a way that they anchor in the region of the head-group. In contrast, their methoxy congeners cannot anchor effectively and are embedded deeper in the hydrophobic segment of the lipid bilayers. The MD results explain the fact that hydroxystilbenoid analogs exert more significant effects on the pretransition than their methoxy congeners, especially at low concentrations. To maximize the polar interactions, the two phenolic hydroxyl groups are localized in the vicinity of the head-group region, directing the remaining hydroxy group in the hydrophobic region. This topographical position of stilbenoid analogs forms a mismatch that explains the significant broadening of the width of the phase transition and lowering of the main phase-transition temperature in the lipid bilayers. At high concentrations, hydroxy and nonhydroxy analogs appear to form different domains. The correlation of thermal effects with antioxidant activity is discussed.

Keywords DPPC · DSC · Molecular dynamics · Resveratrol analogs · Stilbenes

Introduction

The importance of the role of membranes in antioxidant activity is well established. Resveratrol is found to be located in the lipid region of the bilayer close to the double bonds of polyunsaturated fatty acids, making them suitable for prevention and control of lipid peroxidation of the membranes (Fabris et al. 2008).

In the past, we have published a series of papers in which the role of phenolic hydroxyl group of cannabinoids

(CBs) has been studied (Mavromoustakos et al. 1991; 1995a, b; 1996a, b; Yang et al. 1992). It is well known that phenolic hydroxyl groups in the CB family play a pivotal role in their bioactivity. In the published research work the thermal and dynamic properties of CB analogs possessing phenolic hydroxyl group were compared with the corresponding methylated analogs. We found distinct differential thermal effects, dynamics, and localization in lipid bilayers of CBs possessing a hydroxyl group, when compared with those lacking such a group. Surprisingly, molecules possessing a phenolic hydroxyl group affected lipid bilayers more significantly than the corresponding methylated analogs. In particular, CB analogs possessing a phenolic hydroxyl group lowered and broadened the phase-transition temperature more significantly at identical molar fractions in comparison with identical molecules differing only in the methylation of the phenolic hydroxyl group. X-ray and neutron diffraction studies have shown different topographical location in lipid bilayers, and solid-state ^2H nuclear magnetic resonance (NMR) showed different orientation. Molecules possessing a phenolic hydroxyl group are localized in the interface of the lipid bilayers, with the phenolic hydroxyl group probably hydrogen-bonding either with the head-group or the glycerol carbonyls. The methylated analogs locate themselves deeper in the hydrophobic region since they lack the anchor for the polar region (Guo et al. 2008; Martel et al. 1993; Mavromoustakos et al. 1991; 1995a, b; 1996a, b; 1998; 1999; 2001; Sarpietro et al. 2007, Yang et al. 1993).

In this paper, we describe an extension of our work with synthetic analogs of resveratrol in an attempt to gain more insight into the role of phenolic hydroxyl groups on the effects that bioactive molecules have in lipid bilayers. The aim of this study is twofold: (1) to answer the question of the generalization of the thermal effects of compounds possessing phenolic hydroxyl groups, and (2) to examine the effect of the modification of the phenolic hydroxyl group. To achieve these objectives, we synthesized several analogs possessing phenolic hydroxyl groups together with their methylated congeners. While our work was in progress, a similar, more limited study appeared in the literature where only resveratrol, 3,5,4'-tri-*O*-methylresveratrol, and 3,5,4'-tri-*O*-acetylresveratrol were evaluated (Sarpietro et al. 2007). Of special interest are the results reported for resveratrol and its trimethylated analog: (a) Resveratrol caused suppression of the pretransition at all molar fractions used, while with trimethylresveratrol the same effect was observed for concentrations higher than $x = 0.015$, indicating that it probably localizes in the nonpolar region of the lipid bilayers; (b) Increasing the molar fraction of resveratrol caused a gradual shift towards a lower main phase-transition temperature and broadening of the phase transition, indicating a decrease of the cooperativity of the main transition

and the induction of disorder on the structural lipid; resveratrol caused stronger lowering of the phase-transition temperature than trimethylresveratrol, but the latter exerted stronger broadening of the width of the phase transition than the former at $x \geq 0.15$; (c) Phase separation was observed for resveratrol at $x = 0.09$, while trimethylresveratrol did not show a well-defined phase separation; resveratrol was reported to form concentration-rich and concentration-poor domains; (d) Partition studies showed a high percentage of the two molecules in lipid bilayers (90% for resveratrol and 99.16% for the trimethylated analog); (e) Kinetic studies showed that only resveratrol was taken up by the biomembrane model, whereas exogenous uptake of the trimethylated analog was very poor; (f) While the trimethylated analog showed reduced mobility in aqueous medium when it is exogenously incorporated, it is effectively taken up by biomembranes when the aqueous barrier is overcome.

In a recent publication the effects of resveratrol and picetamol in model bilayers were studied using electron spin resonance, fluorescence, and differential scanning calorimetry (DSC). These studies showed preferential interaction of resveratrol and picetamol with the head-group region of lipid bilayers (Wesolowska et al. 2009).

In our study, DSC was used for a series of 13 synthetic stilbenoid molecules (Fig. 1) incorporated in dipalmitoylphosphatidylcholine (DPPC) bilayers at various molar fractions. These molecules constitute derivatives of resveratrol (compound 1 in Fig. 1) with one or more of the following characteristics: (1) the ring possessing only one phenolic hydroxyl group has in the *ortho* position either *tert*-butyl (*t*-Bu) or 1-ethyl-propyl substituents (-CHEt₂); (2) the coupling of the two aromatic rings is extended by another olefinic double bond; (3) the phenolic hydroxyl groups are methylated. Such a series of synthetic analogs allowed us to study not only the role of phenolic hydroxyl and methoxy groups but also (1) the *ortho* substitution effect of lipophilic segments and (2) the effect of elongation of the conjugation between the two phenyl rings.

Materials and methods

The phenolic stilbene derivatives were obtained by demethylation of the corresponding *O*-methyl analogs synthesized using the Horner–Wadsworth–Emmons reaction.

The syntheses of compounds 3, 4, 7, and 8 (Skretas et al. 2007) and 5, 6, and 9–14 have been described (Villalonga-Barber et al. 2011). Compound 2 (Privat et al. 2002) was prepared using the procedure described by Villalonga-Barber et al. (2011) for synthesis of *trans*-stilbene derivatives, while the synthesis of resveratrol has been described by Privat et al. (2002).

Lipophilicity was expressed by the octanol–water partition coefficients, calculated by means of ClopP software version 4.0 (BioByte, Claremont CA, USA) for Windows. Structures were introduced in SMILES format. $C \log P$ is based on the Leo–Hansch fragmental system (Leo and Hoekman 2000). Calculated values of $C \log P$ are presented in Fig. 1, which also includes differences in lipophilicity between pairs of compounds.

Differential scanning calorimetry (DSC)

L_α -DPPC (99 + %) was purchased from Avanti Polar Lipids Inc. (Alabaster, AL) and spectroscopic-grade CHCl_3 from Sigma–Aldrich (St. Louis, MO). Appropriate amounts of L_α -DPPC and the studied synthetic molecules were diluted in chloroform, mixed and then dried under a stream of N_2 , and stored under vacuum overnight. After dispersion in water (50% w/w), portions of the samples (ca. 5 mg) were sealed in stainless-steel capsules obtained from

PerkinElmer (Norwalk, CT). Thermal scans were obtained using a PerkinElmer DSC-7 calorimeter. All samples were scanned from 10°C to 60°C until identical thermograms were obtained, using scanning rate of 2.5°C/min. The temperature scale of the calorimeter was calibrated using indium ($T_m = 156.6^\circ\text{C}$) and DPPC bilayers ($T_m = 41.2^\circ\text{C}$).

The following diagnostic parameters in the observed endothermic events were recorded during the phase transition and are used for the study of drug–membrane interactions: T_m (maximum of the temperature peak), T_{onset} (starting temperature of the phase transition), and $T_{m1/2}$ (full-width at half-maximum of the phase transition). The area under the peak represents the enthalpy change during the transition (ΔH).

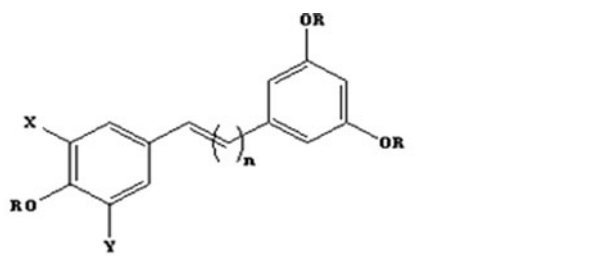
A baseline for an empty pan as a reference and a sample containing double-distilled water was run for the temperature range of 10–60°C. For a given temperature range, the background obtained using the double-distilled water as a reference was subtracted from the thermal scans of the samples containing lipid bilayers with or without drug.

ΔH and T_m values for the pre- and main phase transitions for DPPC bilayers were compared with those obtained in the literature (Koynova and Caffrey 1998). Our values were within those reported in the review ($T_m 34.4 \pm 2.5$ and 41.3 ± 1.8 ; $\Delta H 1.3 \pm 1.0$ and 8.2 ± 1.4 kcal/mol). Mean values of three identical scans are tabulated.

The drug concentrations used in the preparations were $x = 0.01$ (99% molar ratio of phospholipid, 1% molar ratio of drug), $x = 0.05$, $x = 0.10$, and $x = 0.20$.

Molecular dynamics (MD) simulations

The DPPC lipid bilayer for the MD simulations was adopted from Dr. M. Karttunen's webpage (Patra et al. 2004): 128 DPPC lipids and 3,655 water molecules after 100 ns; (Kandt et al. 2007; Patra et al. 2003). The MD simulations were performed using the GROMACS 3.3.1 software package (Lindhal et al. 2001) using the GRO-MOS96 force field (Van Gunsteren et al. 1996). Two representative compounds were used: compounds **2** and **14**. Simulations were performed for different concentrations of compounds in the DPPC lipid bilayers using only one representative compound (either compound **2** or compound **14**) and six molecules (six molecules of compound **2** or six molecules for compound **14**); for the MD simulations of high drug concentrations, half of them were used in one DPPC layer and the others were used in another layer. Ligands were merged to the lipid bilayers as discussed in the “Results and discussion” section. Lipids clashing with the ligands were removed from the simulation. For example, 88 DPPC lipids and 3,655 water molecules were used for the MD simulations of high drug concentration at DPPC. Simulations were run in the isobaric-isothermal



Compound	R	X	Y	n	$C \log P$	Pair	Diff
1	H	H	H	1	2.43		
2	CH_3	H	H	1	3.02	0.53	
3	H	t-Bu	H	1	4.26		
4	CH_3	t-Bu	H	1	4.85	0.59	
5	H	$\text{CH}(\text{Et})_2$	H	1	4.72		
6	CH_3	$\text{CH}(\text{Et})_2$	H	1	5.50	0.78	
7	H	H	H	2	3.04		
8	CH_3	H	H	2	3.62	0.58	
9	H	t-Bu	H	2	4.86		
10	CH_3	t-Bu	H	2	5.45	0.58	
11	H	$\text{CH}(\text{Et})_2$	H	2	5.32		
12	CH_3	$\text{CH}(\text{Et})_2$	H	2	6.11	0.79	
13	H	$\text{CH}(\text{Et})_2$	$\text{CH}(\text{Et})_2$	1	7.00 *		
14	H	$\text{CH}(\text{Et})_2$	$\text{CH}(\text{Et})_2$	2	7.61 *	0.61	

* Too high values to be realistic in nature

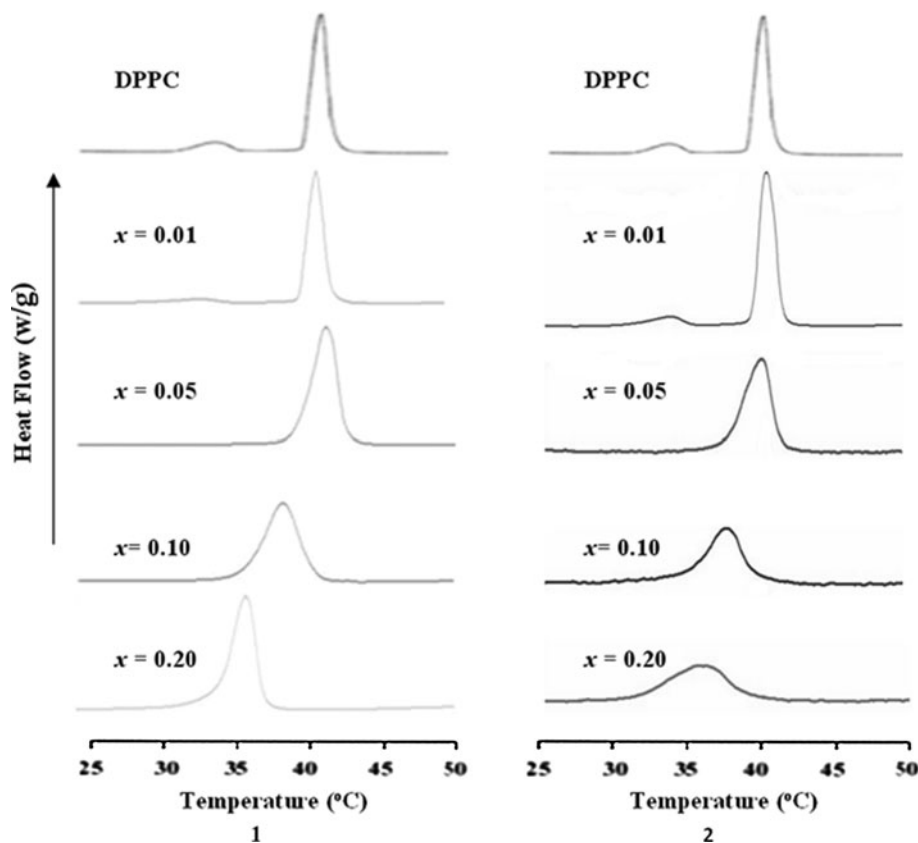
Fig. 1 Compounds used in the study, calculated $C \log P$ values, and the differences in lipophilicity between pairs of compounds

(*NPT*) ensemble at 300 K and 1 bar with periodic boundary conditions. During equilibration, the Berendsen barostat and thermostat algorithms (Berendsen et al. 1984) were applied. Electrostatic interactions were calculated using the particle mesh Ewald method (Essmann et al. 1995). Cutoff distances for the calculation of Coulomb and van der Waals interactions were 10 and 14 Å, respectively. Prior to the dynamics simulation, energy minimization was applied to the full system without constraints using a steepest-descent integrator for 2,000 steps with initial step size of 0.01 Å [minimization tolerance set to 1,000 kJ/(mol.nm)]. The system was then equilibrated by 250 ps (for high drug concentrations at the lipid bilayer simulations this value was set to 0.5 ns) simulation with time step of 2 fs; subsequently, a 2.5 ns (for high drug concentrations at the lipid bilayer simulations this value was set to 3.0 ns) simulation was performed at 300 K and 1 bar with time step of 2 fs using Berendsen thermostat and Parrinello-Rahman barostat algorithms (Parrinello and Rahman 1981). All bonds were constrained using the LINCS algorithm (Hess et al. 1997).

Results and discussion

As a first set of compounds for comparison, we used resveratrol (**1**) and its trimethylated analog (**2**, Fig. 2). Our

Fig. 2 Differential scanning calorimetry thermograms of DPPC, DPPC + **1**, and DPPC + **2** at $x = 0.01$, $x = 0.05$, $x = 0.10$, and $x = 0.20$ using scanning rate of 2.5°C/min



results in DPPC bilayers resembled those reported with DMPC bilayers by Sarpietro et al. In particular, at $x = 0.01$, resveratrol almost suppressed the pretransition while the trimethylated analog exerted a less pronounced effect. At higher concentrations, both molecules caused suppression of the pretransition temperature. Resveratrol caused more effective lowering of the main phase transition than its trimethylated analog, while the latter at higher molar fractions caused more significant broadening. Pretransition suppression is frequently observed when a drug molecule is incorporated in lipid bilayers (Kyrikou et al. 2004a, b; Mavromoustakos et al. 1997; Zoumpoulakis et al. 2003). This is attributed to perturbation of the head-group. The presence of the drug molecule affects the conformational properties of the head-group in phosphatidylcholine bilayers. The relationship of the head-group structures with the pretransition has already been reported in the literature; for example, dipalmitoylphosphatidyl ethanolamine (DPPE) bilayers contain ethanolamine instead of choline as a head-group and do not show pretransition in their thermal scans (Houslay and Stanley 1982). Phase separation for the two compounds such as that reported with DMPC bilayers was not obvious. The trimethylated analog showed identical ΔH at $x = 0.01$ and lower ΔH at higher concentrations (Table 1). Comparison of the results with those obtained using CB analogs show that a generalization for the two different classes cannot be

Table 1 Thermodynamic parameters T_{onset} , T_m , $T_{m1/2}$, and ΔH for the differential scanning calorimetry scans

	Conc.	T_{onset}	T_m	T_m	T_m	$T_{m1/2}$	$T_{m1/2}$	ΔH (kcal/mol)	ΔH (kcal/mol)
DPPC		32.6	40.2	34.7	41.2	2.0	1.2	1.09	8.18
1	+ x = 0.01	27.4	39.8	31.1	40.7	4.1	1.1	0.61	8.03
	+ x = 0.05	–	39.6	–	41.7	–	2.3	–	7.76
	+ x = 0.1	–	36.1	–	38.3	–	2.3	–	8.27
	+ x = 0.2	–	34.4	–	36.0	–	2.4	–	8.88
2	+ x = 0.01	31.0	39.5	33.7	40.3	2.4	1.3	–	7.83
	+ x = 0.05	–	37.8	–	40.0	–	2.1	–	7.00
	+ x = 0.1	–	35.1	–	37.6	–	2.5	–	5.95
	+ x = 0.2	–	31.2	–	35.7	–	4.4	–	6.80
3	+ x = 0.01	–	39.4	–	40.5	–	1.4	–	8.18
	+ x = 0.05	–	38.4	–	40.0	–	1.5	–	7.9
	+ x = 0.1	–	35.0	–	37.8	–	2.55	–	7.57
	+ x = 0.2	–	29.0	–	30.4	–	2.95	–	8.01
4	+ x = 0.01	29.7	39.5	32.9	40.9	3.65	1.48	0.63	7.94
	+ x = 0.05	–	37.0	–	40.4	–	1.9	–	7.09
	+ x = 0.1	–	33.1	–	39.0	–	4.0	–	7.87
	+ x = 0.2	–	28.0	–	34.5	–	7.2	–	7.94
5	+ x = 0.01	–	39.8	–	41.2	–	1.45	–	7.92
	+ x = 0.05	–	38.3	–	40.0	–	1.85	–	7.87
	+ x = 0.1	–	35.2	–	38.2	–	3.19	–	8.01
	+ x = 0.2	–	26.8	–	29.8	–	6.25	–	8.15
6	+ x = 0.01	29.1	39.7	32.2	41.0	3.6	1.25	0.39	7.8
	+ x = 0.05	–	38.2	–	40.5	–	2.1	–	8.01
	+ x = 0.1	24.3	34.7	24.7	38.6	2.85	4.2	0.05	8.29
	+ x = 0.2	25.3	32.8	26.5	37.0	2.75	4.65	0.51	7.92
7	+ x = 0.01	–	40.0	–	40.9	–	1.23	–	7.92
	+ x = 0.05	–	39.0	–	39.3	–	1.33	–	7.99
	+ x = 0.1	–	36.5	–	38.5	–	1.85	–	7.67
	+ x = 0.2	–	33.7	–	35.5	–	2.0	–	9.17
8	+ x = 0.01	31.4	40.0	34.1	41.2	2.26	1.4	1.02	8.20
	+ x = 0.05	28.1	38.4	30.9	39.7	3.1	1.26	0.67	7.67
	+ x = 0.1	–	37.4	–	39.0	–	1.65	–	6.71
	+ x = 0.2	–	36.6	–	38.8	–	2.48	–	6.83
9	+ x = 0.01	–	40.0	–	41.0	5.0	1.7	–	7.97
	+ x = 0.05	–	38.3	–	40.0	–	1.6	–	7.74
	+ x = 0.1	–	34.4	–	38.0	–	3.8	–	8.25
	+ x = 0.2	–	24.2	–	27.0	–	5.2	–	8.53
10	+ x = 0.01	29.2	39.6	32.9	40.8	5.2	1.25	0.68	7.87
	+ x = 0.05	–	38.4	–	40.0	–	1.7	–	7.48
	+ x = 0.1	–	36.2	–	39.6	–	3.13	–	7.52
	+ x = 0.2	–	31.6	–	36.3	–	4.88	–	5.71
11	+ x = 0.01	–	39.6	–	40.9	–	1.25	–	8.29
	+ x = 0.05	–	39.0	–	40.4	–	1.45	–	8.03
	+ x = 0.1	–	33.7	–	37.8	–	4.5	–	8.6
	+ x = 0.2	–	23.7	–	25.6	–	9.4	–	8.71

Table 1 continued

	Conc.	T_{onset}	T_m	$T_{m1/2}$	ΔH (kcal/mol)				
12	+ $x = 0.01$	29.6	39.2	32.5	40.5	3.9	1.2	0.61	7.78
	+ $x = 0.05$	–	37.9	–	39.7	–	1.7	–	7.97
	+ $x = 0.1$	–	35.3	–	39.1	–	3.3	–	7.76
	+ $x = 0.2$	–	34.9	–	38.4	–	3.3	–	7.55
13	+ $x = 0.01$	28.4	40.1	32.0	40.9	3.5	1.3	0.5	7.9
	+ $x = 0.05$	–	38.1	–	39.9	–	1.9	–	7.6
	+ $x = 0.1$	–	32.8	–	39.2	–	6.3	–	5.7
	+ $x = 0.2$	–	30.5	–	35.9	–	6.0	–	2.7
14	+ $x = 0.01$	28.8	40.1	32.2	41.3	3.4	1.2	0.5	7.9
	+ $x = 0.05$	–	38.1	–	40.1	–	1.8	–	7.6
	+ $x = 0.1$	–	34.1	–	37.5	–	5.3	–	6.2
	+ $x = 0.2$	–	28.0	–	35.4	–	6.5	–	4.7

achieved. The thermal scans of lipid bilayers containing CB analogs possessing a phenolic hydroxyl group, especially at high concentrations, contain very broad multi-component peaks, whereas this is not observed with resveratrol and its derivatives. The methylated CB analogs also show lesser thermal effects compared with the trimethylated stilbenoid analogs, especially at high concentrations. However, the general trend is the same. Both CB and stilbenoid analogs suppress the pretransition temperature at low concentrations, lower the phase-transition temperature, and significantly broaden the phase transition in a concentration-dependent manner. At high concentrations, “domains” are observed, indicating uneven distribution of the molecules in the lipid bilayers.

These observations are significant because it appears that DSC scans are very sensitive not only to the presence of a phenolic hydroxyl group or its methylated derivative but to other structural details as well. This fact urged us to examine more synthetic analogs and consider the modification of their thermal effects.

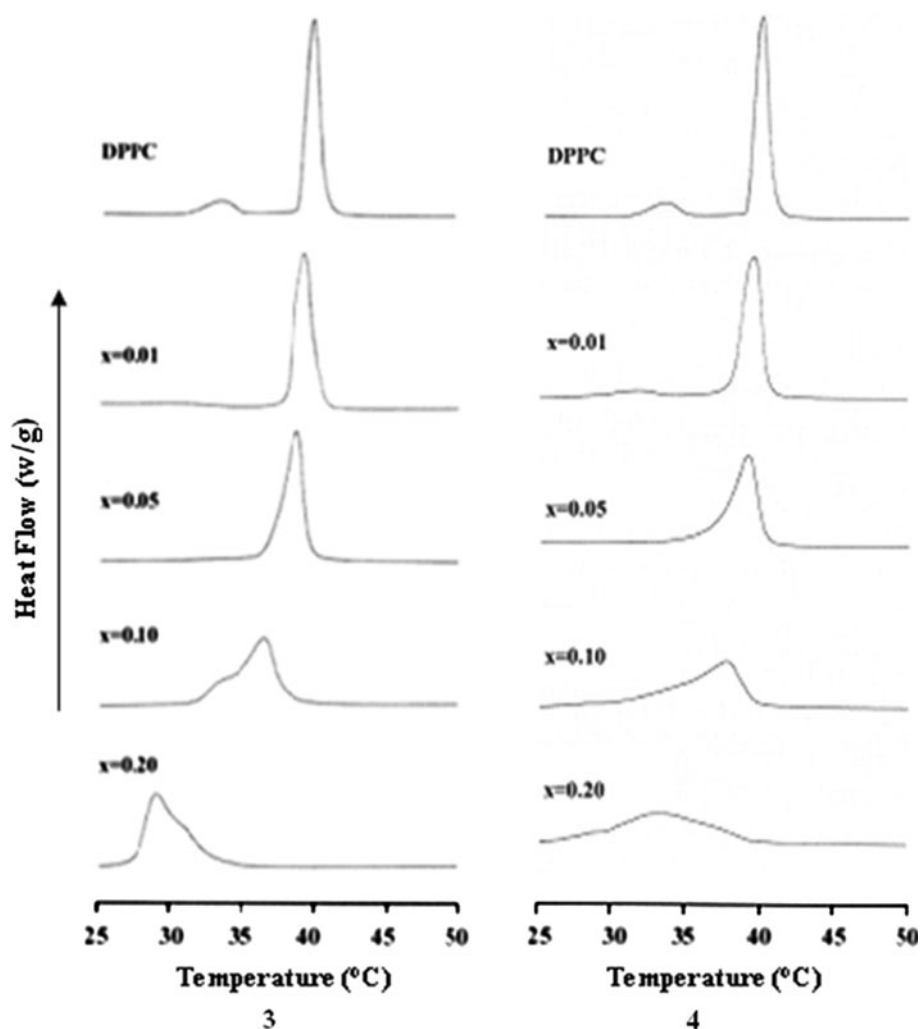
The second set of stilbenoid analogs for comparison (**3** and **4**, Fig. 3) contains a *t*-Bu group (X substituent) *ortho* to the -OH or -OCH₃ group. At $x = 0.01$ the hydroxylated analog **3** suppresses the pretransition and **4** affects it significantly by broadening it. At higher concentrations, both exert suppression of the pretransition. At $x = 0.01$, both molecules affect the width of the pretransition more in comparison with the nonalkylated compounds **1/2** couple. At $x \geq 0.10$, the hydroxyl-bearing analog shows phase separation as the transition peak clearly indicates at least two components. As with compounds **1** and **2**, the hydroxylated analog causes more effective lowering of the phase transition and, at concentrations of $x \geq 0.10$, less broadening. In comparison with **1** and **2** the broadening and lowering of the phase-transition temperature is more prominent. This is attributed to the *t*-Bu group. Such a

bulky group may compel the monohydroxylated ring to locate away from the polar region. The phenolic hydroxyl group is forced to be situated in a less favorable, more lipophilic environment where the *t*-Bu group has more affinity, and this mismatch causes phase separation. Above a critical concentration, the molecules are probably positioned into two different and distinct localizations in lipid bilayers. Different domains are therefore formed due to the different localization of the drug molecules in the lipid bilayers. Thus, the gradual increase of the width in the phase transition is attributed to two factors: (i) increase of incorporation; and (ii) effective mismatch. This hypothesis, as we will discuss later, is strengthened by the MD experiments and $C \log P$ calculations.

In the third set of two compounds (**5** and **6**, Fig. 4) the *t*-Bu group is replaced by a 1-ethyl-propyl substituent. As expected, the thermal profiles for **5** and **6** are very similar to those observed for **3** and **4**. However, it should not escape our notice that there are significant differences between the two sets of compounds **3/4** and **5/6** at the high concentration of $x = 0.20$. Generally, thermal scans at high concentrations are very sensitive to experimental conditions, and the formation of domains is not fully reproducible (Mavromoustakos et al. 1995b). Similar conclusions have been obtained for the other four pair of analogs **7/8**, **9/10**, **11/12**, and **13/14** (see Fig. SF1–SF4 in the Supplementary Material).

It has been previously reported that the proper conformation, orientation, and location of a drug molecule in the membrane are critical for it to reach its site of action and interact productively with that site (Fotakis et al. 2010; Kyrikou et al. 2004a, b; Martel et al. 1993; Mavromoustakos et al. 1994; 1995a, b, 1997; Zoumpoulakis et al. 2003). To investigate the orientation of the studied molecules in the DPPC bilayers, MD simulations have been applied. For this study, two representative compounds are

Fig. 3 Differential scanning calorimetry thermograms of DPPC, DPPC + **3**, and DPPC + **4** at $x = 0.01$, $x = 0.05$, $x = 0.10$, and $x = 0.20$ using scanning rate of $2.5^\circ\text{C}/\text{min}$



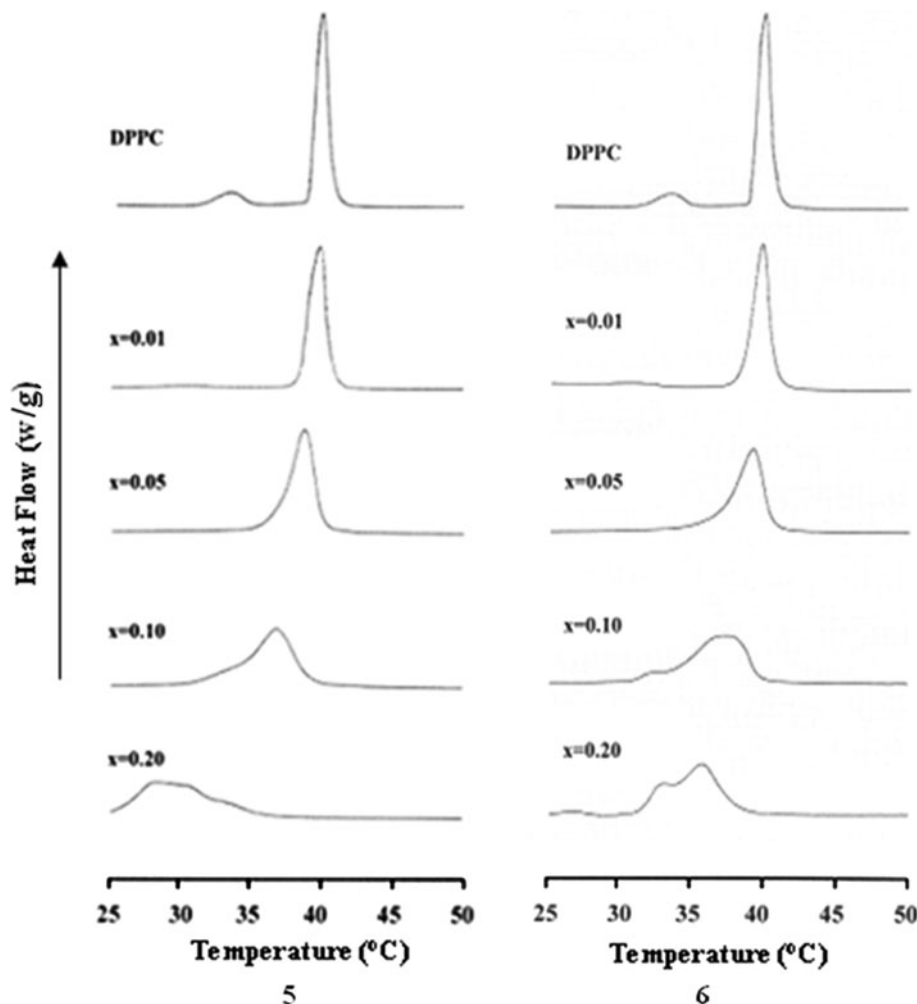
selected for discussion: the methyl analog of resveratrol **2** and compound **14**. Studies showed identical results using two different drug concentrations in the lipid bilayer (either one molecule or six molecules in the lipid bilayer). The two molecules were initially placed in an identical position and orientation (the lipophilic segment of the molecules approximately parallel to the bilayer normal) in the bilayer and then subjected to MD (Fig. 5).

Figure 6 shows the radial distribution function (RDF) between oxygen atoms of ligands and phosphorus atoms of lipid bilayers. While compound **14** is packed perfectly in the vicinity of the head-groups of the lipid bilayer ($\sim 5 \text{ \AA}$), compound **2** does not locate in the realm of the head-group (Figs. 5, 7). The two hydroxyl groups (oxygen numbering O14 and O16) of compound **14** (Fig. 7b) are not restricted by any alkyl branching on the compound, and this part of ligand can reach the polar head-groups of lipid (i.e., blue and black lines in the RDF plot, Fig. 6b). The red line in this plot represents the distribution of O15 of ligand **14** with the lipids, where the alkyl substituents restrain its distribution with the head-groups of the lipid bilayer (it is

observed that the red line does not have a sharp peak, showing no pair distribution). The RDF plot for compound **2** does not have sharp peaks (Fig. 6a). O19 of compound **2** distributes closer to the head-groups of the lipid bilayer compared with O15 and O17.

MD results show that molecules that possess phenolic hydroxyl groups orient in the lipid bilayers in an awkward orientation with their long axis such that the majority of the hydroxy groups anchor in the realm of the head-group. In contrast, their methoxy congeners orient with the long axis perpendicular to the plane of the lipid bilayers. Calculation of values for the seven pairs of analogs supports this interpretation. For all pairs used, methylated analogs had higher $C \log P$ (ranging between 0.53 and 0.79) than the corresponding hydroxyl stilbenoid congeners (Fig. 1). Such an orientation was also observed for the corresponding CB analogs. These MD results explain the fact that hydroxylated molecules exert more significant effects on the pretransition than their methoxy congeners, especially at low concentrations. This awkward orientation observed for the hydroxylated molecules maximizes the

Fig. 4 Differential scanning calorimetry thermograms of DPPC, DPPC + **5**, and DPPC + **6** at $x = 0.01$, $x = 0.05$, $x = 0.10$, and $x = 0.20$ using scanning rate of $2.5^\circ\text{C}/\text{min}$



polar interactions but leaves the remaining hydroxyl group to be embedded in the hydrophobic region. This mismatch explains the greater broadening of the width of the phase transition and lowering of the main phase-transition temperature. At high concentrations, hydroxylated and non-hydroxylated compounds appear to form different domains. This is also explained by MD calculations which show several topographical locations (i.e., distribution in the upper and lower segments of the lipophilic core) for the compounds in the lipid bilayers. The different locations expressed as different domains result in broad multicomponent thermal scans.

MD calculations confirm the DSC experimental observations. The analogs that contain phenolic hydroxyl groups affect the pretransition temperature more significantly because they anchor in the head-group region. In addition, the distribution results explain the significant broadening and formation of domains of the two compounds due to the mismatch of polar and nonpolar interactions.

Experimental data showed that only hydroxylated analogs possess neuroprotective antioxidant activity

(Villalonga-Barber et al. 2011). This neuroprotective activity was more evident for molecules possessing alkyl substituents on their aromatic rings, with derivatives with two alkyl substituents outperforming those with one such group, presumably as a result of higher stabilization of the respective aroxyl radical. Interestingly, the most potent derivatives displayed $C \log P$ values in the range 6.3–7.6, which is higher than that usually seen with most drugs, likely reflecting the need for increased placement into plasma and/or mitochondrial membranes to improve potency. We reasoned that lipophilic antioxidants are likely to be more capable of reaching sites of reactive oxygen species (ROS) production inside mitochondria (Villalonga-Barber et al. 2011). The DSC and MD data can provide a mechanistic basis in support of this observation, since they propose a mode of placement of the stilbenoid derivatives in lipid bilayers that is correlated with the differences in their neuroprotective potency. Methylated analogs are embedded deeper in the hydrophobic segment of the lipid bilayers and cannot exert any action on the polar interface. Stilbenoid hydroxylated analogs, on the other hand,

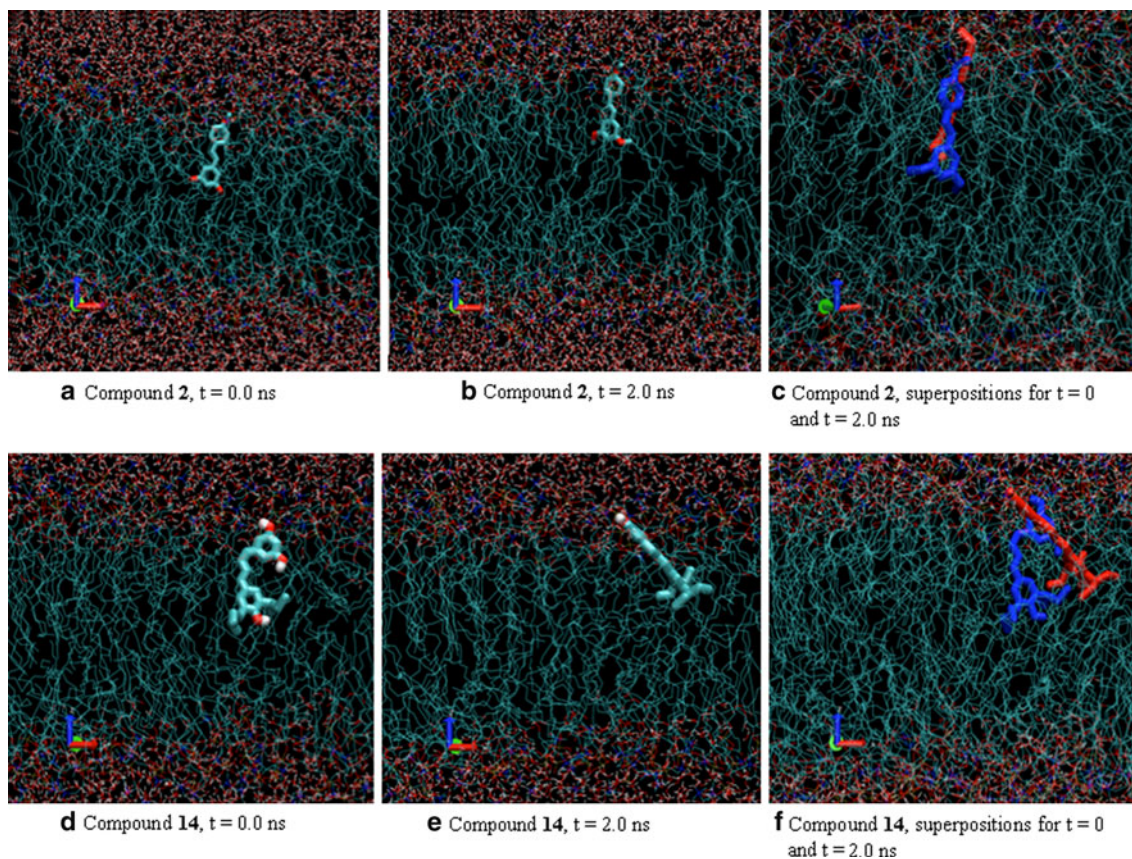


Fig. 5 Orientations of trimethylated analog of resveratrol (compound **2**) and compound **14** within the bilayer before ($t = 0$ ns) and after ($t = 2$ ns) MD simulations. In addition to initial and final conformations of compounds at the lipid bilayer environment, superimpositions

of initial and final conformations are also depicted for clarity (**d** and **f**). *Top* (**a–c**) and *bottom* (**d–f**) figures represent topological changes of compounds **2** and **14**, respectively, at the lipid bilayer

because they bear phenolic hydroxyl “anchors”, are positioned in the interface of the lipid bilayers. When these polyphenolic analogs possess alkyl substituents, the molecules are oriented in an awkward way, i.e., with their long axis almost parallel to the bilayer plane, in order to maximize the polar interactions. The molecules still have an accessible phenolic hydroxyl group in the upper part of the lipophilic segment. This group may serve to prevent lipid hyperoxidation when unsaturated lipids are present in the lipid bilayers. As shown for α -tocopherol in a recent review article, this is a suitable position to exert its antioxidant action (Atkinson et al. 2008). Firstly, it communicates with the polar region and exerts a possible interaction with ascorbic acid, and secondly, it interacts with unsaturated parts of the lipids and prevents hyperoxidation. A similar membrane location and phenolic hydroxyl function has been also proposed to account for the antioxidant neuroprotective activity of 17β -estradiol based on rotational-echo double-resonance NMR studies of interaction of the hormone and analogs thereof with DPPC phospholipid multilamellar vesicles (Cegelski et al. 2006). Estradiol is thought to intercalate into the neuronal plasma and

mitochondrial membranes with its phenolic ring positioned near the site of lipid peroxidation, thus preventing oxidative stress-induced collapse of ion gradients and mitochondrial energy production failure, known to result in damage of the organelle and cell death (reviewed by Simpkins et al. 2010).

Conclusions

In this research work, modifications of thermal effects caused by synthetic polyphenolic stilbenoids and their methylated congeners on lipid bilayers have been studied to provide more information concerning the effect of phenolic hydroxyl groups and their methylated analogs. Previous studies showed that CBs bearing a phenolic hydroxyl group modify the thermal properties of lipid bilayers more significantly than the methoxy analogs, and these effects were attributed to the fact that, while phenolic hydroxyl groups anchor in the region of the lipid bilayer head-group, the methoxy analogs are embedded deeper towards the hydrophobic region.

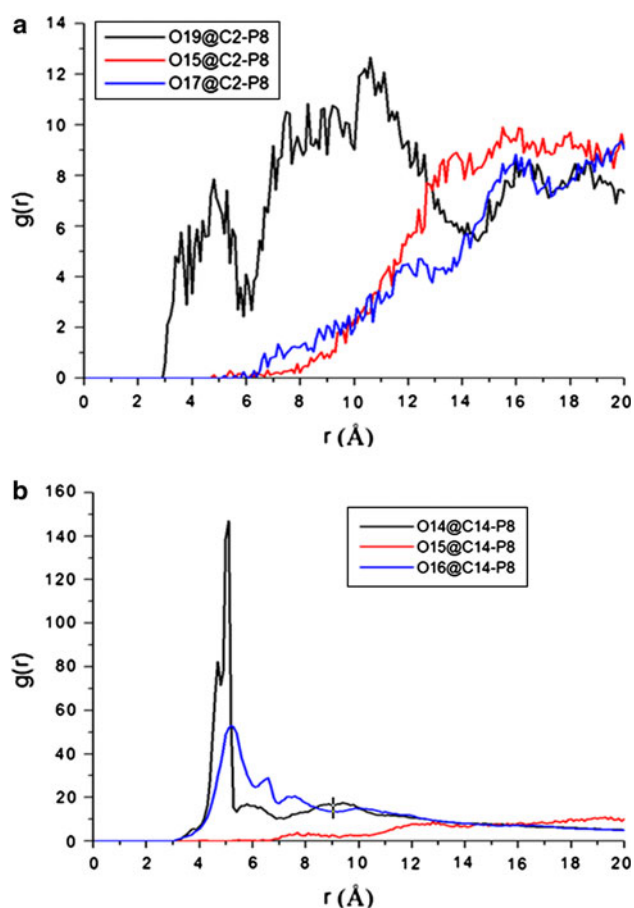


Fig. 6 Radial distribution functions of oxygen atoms (O15, O17, and O19) and phosphorus atoms (P8) of lipid bilayers throughout the simulations **(a)** for compound **2** and **(b)** for compound **14**. Figures are generated by the derived MD trajectory files for both ligands using the VMD program. For numbering of oxygen atoms in the ligands see Fig. 7

Although, in general, a similar picture emerges from this study, some subtle differential thermal effects lead to further understanding of the phenolic hydroxyl groups. The analogs possessing phenolic hydroxyl groups generally modify the effects of lipid bilayers more significantly, but this is not as pronounced as with the CBs. In addition, at high concentrations, both analogs exert similar thermal effects expressed as broadening of the width of the phase transition temperature and lowering of the phase transition and cause of phase separation.

To further generalize our observations on the two classes of molecules, it appears that, when drug molecules are forced to act on the interface through membrane perturbation, phenolic hydroxyl groups can serve as anchors to achieve this purpose. This information could be of benefit for synthetic chemists who are seeking to design molecules which act on the interface region of the membranes. An additional and potentially useful design factor which arises from this study is that molecules possessing a mismatch of

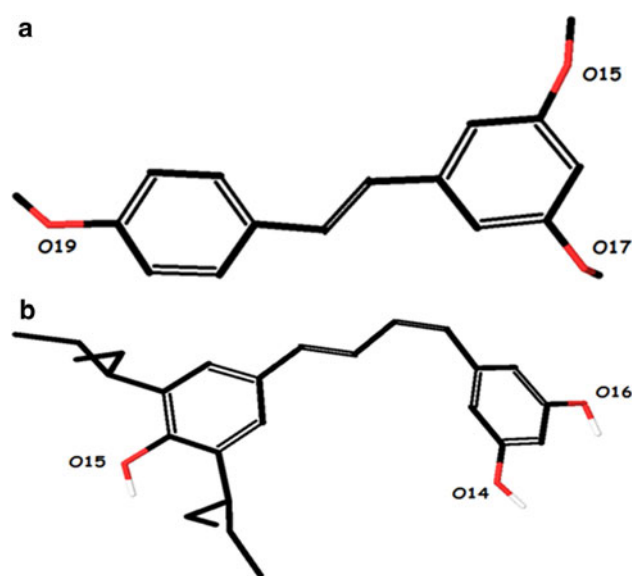


Fig. 7 Oxygen atom numbering for the ligands: **a** compound **2**, and **b** compound **14**

substituents in the vicinity of lipophilic region are able to significantly perturb the lipid bilayer.

Acknowledgments This work was supported in part by the EU Marie Curie Host Fellowship for Early Stage Research Training (EST) Programme MEST-CT-2005-020575 and a Center of Excellence Research program from the General Secretariat for Research and Technology. C. Koukoulitsa is a recipient of a Hrakleitos II scholarship.

References

- Atkinson J, Epand RF, Epand RM (2008) Tocopherols and tocotrienols in membranes. A critical review. *Free Radic Biol Med* 44:739–764
- Berendsen HJC, Postma JPM, van Gunsteren WF, Dinola A, Haak JR (1984) Molecular dynamics with coupling to an external bath. *J Chem Phys* 81:3684–3690
- BioByte Corp., 201 West 4th St., Suite 204, Claremont, CA 91711, United States
- Cegelski L, Rice CV, O' Connor RD, Caruano AL, Tochtrop GR, Cai ZY, Covey DF, Schaefer J (2006) Mapping the locations of estradiol and potent neuroprotective analogues in phospholipid bilayers by REDOR. *Drug Dev Res* 66:93–102
- Essmann U, Perera L, Berkowitz ML, Darden T, Lee H, Pedersen LG (1995) A smooth particle mesh Ewald method. *J Chem Phys* 103:8577–8592
- Fabris S, Federico M, Giampietro R, Stevanato R (2008) Antioxidant properties of resveratrol and piceid on lipid peroxidation in micelles and monolamellar liposomes. *Biophys Chem* 125:76–83
- Fotakis C, Gega S, Siapi E, Potamitis C, Viras K, Moutevelis-Minakakis P, Kokotos G, Durdagi S, Grdadolnik S, Sartori B, Rappolt M, Mavromoustakos T (2010) Drug interactions at the bilayer interface and receptor site induced by the novel synthetic pyrrolidinone analog MMK3. *Biochim Biophys Acta* 1798:422–432

- Guo J, Yang D, Chari R, Tian X, Pavlopoulos S, Lu D, Makriyannis A (2008) Magnetically aligned bicelles to study the orientation of lipophilic ligands in membrane bilayers. *J Med Chem* 41:6793–6799
- Hess B, Bekker H, Berendsen HJC, Fraaije JGEM (1997) LINC: a linear constraint solver for molecular simulations. *J Comput Chem* 18:1463–1472
- Houslay MD, Stanley KK (1982) Dynamics of biological membranes. Wiley, New York
- Kandt C, Ash WL, Tieleman DP (2007) Setting up and running molecular dynamics simulations of membrane proteins. *Methods* 41:475–488
- Koynova R, Caffrey M (1998) Phases and phase transitions of the phosphatidylcholines. *Biochim Biophys Acta* 1376:91–145 (and reference therein)
- Kyrikou I, Hadjikakou SK, Kovala-Demertzi D, Viras K, Mavromoustakos T (2004a) Effects of non-steroid anti-inflammatory drugs in membrane bilayers. *Chem Phys Lipids* 132:157–169
- Kyrikou I, Daliani I, Mavromoustakos T, Maswadeh H, Demetzos C, Hatziantoniou S, Giatrellis S, Nounesis G (2004b) The modulation of thermal properties of vinblastine by cholesterol in membrane bilayers. *Biochim Biophys Acta* 1661:1–8
- Leo A, Hoekman D (2000) Calculating log P(oct) with no missing fragments; the problem of estimating new interaction parameters. *Perspect Drug Discov Design* 18:19–38
- Lindhal E, Hess B, van der Spoel D (2001) GROMACS 3.0: a package for molecular simulation and trajectory analysis. *J Mol Model* 7:306–317
- Martel P, Makriyannis A, Mavromoustakos T, Kelly K, Jeffrey KR (1993) Topography of tetrahydrocannabinol in model membranes using neutron diffraction. *Biochim Biophys Acta* 1151:51–58
- Mavromoustakos T, Daliani I (1999) Effects of cannabinoids in membrane bilayers containing cholesterol. *Biochim Biophys Acta* 1420:252–265
- Mavromoustakos T, Theodoropoulou E (1998) A combined use of ^{13}C -cross polarization/magic angle spinning, ^{13}C -magic angle spinning and ^{31}P -nuclear magnetic spectroscopy with Differential Scanning Calorimetry to study cannabinoid-membrane interactions. *Chem Phys Lipids* 92:37–52
- Mavromoustakos T, Yang DP, Broderick W, Fournier D, Herbert LG, Makriyannis (1991) A small angle X-Ray diffraction studies on the topography of cannabinoids in synaptic plasma membranes. *Pharmacol Biochem* 40:547–552
- Mavromoustakos T, Yang D, Makriyannis A (1994) Topography of Alphaxalone and Δ^{16} -alphaxalone in membrane bilayers containing cholesterol. *Biochim Biophys Acta* 1194:69–74
- Mavromoustakos T, Yang DP, Makriyannis A (1995a) Small angle x-ray diffraction and differential scanning calorimetric studies on O-methyl(-)- Δ^8 -Tetrahydrocannabinol and its 5' iodinated derivative in membrane bilayers *Biochim. Biophys Acta-Biomembranes* 1237:183–188
- Mavromoustakos T, Yang DP, Makriyannis A (1995b) Effects of the anesthetic steroids alphaxalone and its inactive analog Δ^{16} -analog on the thermotropic properties of membrane bilayers. A model for membrane perturbation. *Biochim Biophys Acta* 1239:257–264
- Mavromoustakos T, De-Ping Yang, Makriyannis A (1996a) Topography and thermotropic properties of cannabinoids in brain sphingomyelin bilayers. *Life Sci* 59:1969–1979
- Mavromoustakos T, Theodoropoulou E, Papahatjis D, Kourouli T, De-Ping Yang, Trumbore M, Makriyannis A (1996b) Studies on the thermotropic effects of cannabinoids on phosphatidylcholine bilayers using differential scanning calorimetry and small angle X-ray diffraction. *Biochim Biophys Acta* 1281:235–244
- Mavromoustakos T, Theodoropoulou E, Yang DP (1997) The use of high-resolution solid-state NMR spectroscopy and differential scanning calorimetry to study interactions of anaesthetic steroids with membrane. *Biochim Biophys Acta* 1328:65–73
- Mavromoustakos T, Papahatjis D, Laggner P (2001) Differential membrane fluidization by active and inactive cannabinoid analogs. *Biochim Biophys Acta* 1512:183–190
- Parrinello M, Rahman A (1981) Polymorphic transitions in single crystals: a new molecular dynamics method. *J Appl Phys* 52:182–190
- Patra M, Karttunen M, Hyvönen M, Falck E, Lindqvist P, Vattulainen I (2003) Molecular dynamics simulations of lipid bilayers: major artifacts due to truncating electrostatic interactions. *Biophys J* 84:3636–3645
- Patra M, Karttunen M, Hyvönen M, Falck E, Vattulainen P (2004) Lipid bilayers driven to a wrong lane in molecular dynamics simulations by subtle changes in long-range electrostatic interactions. *J Phys Chem B* 108:4485–4494
- Privat C, Telo JP, Bernardes-Genisson V, Vieira A, Souchard JP, Nepveu F (2002) Antioxidant properties of *trans-E*-Viniferin as compared to stilbene derivatives in aqueous and nonaqueous media. *J Agric Food Chem* 50:1213–1217
- Sarpietro MG, Spatafora C, Tringali C, Micieli D, Castelli F (2007) Interaction of resveratrol and its trimethyl and triacetyl derivatives with biomembrane models studied by differential scanning calorimetry. *J Agric Food Chem* 55:3720–3728
- Simpkins JW, Yi KD, Yang SH, Dykens JA (2010) Mitochondrial mechanisms of estrogen neuroprotection. *Biophys Acta* 1800:1113–1120
- Skretas G, Meligova A, Villalonga-Barber C, Mitsiou DJ, Alexis MN, Micha-Screttas M, Steele BR, Screttas CG, Wood DW (2007) Engineered chimeric enzymes as tools for drug discovery: generating reliable bacterial screens for the detection, discovery, and assessment of estrogen receptor modulators. *J Am Chem Soc* 129:8443–8457
- Van Gunsteren WF, Billeter SR, Eising AA, Hunenberger PH, Kruger P, Mark AE, Scott WRP, Tironi IG (1996) Biomolecular simulation: the GROMOS96 manual and user guide. Vdf Hochschulverlag
- Villalonga-Barber C, Meligova AK, Alexi X, Steele BR, Kouzinou CE, Screttas CG, Katsanou ES, Micha-Screttas M, Alexis MN (2011) New hydroxystilbenoid derivatives endowed with neuroprotective activity and devoid of interference with estrogen and aryl hydrocarbon receptor-mediated transcription. *Bioorg Med Chem* 19:339–351
- Wesolowska O, Kuzdzal M, Strancar J, Michalak K (2009) Interaction of the chemopreventive agent resveratrol and its metabolite, piceatannol, with model membranes. *Biochim Biophys Acta* 1788:1851–1860
- Yang DP, Mavromoustakos T, Beshah K, Makriyannis A (1992) Amphipathic interactions of cannabinoids with membranes. A comparison between Δ^8 -THC and its O-methyl analog using differential scanning calorimetry, X-ray diffraction and solid state ^2H -NMR. *Biochim Biophys Acta* 1103:25–36
- Yang DP, Mavromoustakos T, Makriyannis A (1993) Small angle X-ray diffraction studies of Δ^8 -tetrahydrocannabinol and its O-methyl analog in membranes. *Life Sci* 53:117–122
- Zoumpoulakis P, Daliani I, Zervou M, Kyrikou I, Siapi E, Lamprinidis G, Mikros E, Mavromoustakos T (2003) Losartan's molecular basis of interaction with membranes and AT_1 receptor. *Chem Phys Lipids* 125:13–25